Nanopatterning of Periodically Strained Surfaces – A Kinetic Monte Carlo Simulation Study

M.I. Larsson[*,**], R.F. Sabiryanov[***], K. Cho[****], and B.M. Clemens[*]

[*]Department of Materials Science and Engineering, Stanford University, Stanford, CA
[**]on leave from Department of Physics, Karlstad University, Sweden
[***]Department of Physics, University of Nebraska at Omaha, Omaha, NE
[****]Department of Mechanical Engineering, Stanford University, Stanford, CA

ABSTRACT

Various aspects of strain-assisted nanopatterning of periodically strained surfaces are investigated using kinetic Monte Carlo simulations. The optimal growth conditions for various material systems can be predicted, as we demonstrate for the model system Co on Pt(111). Both strain relaxation and modified potential energy barriers at step edges, i.e. the Ehrlich-Schwoebel (ES) barriers are found to be of large importance for the nanopatterning.

1 INTRODUCTION

Engineering of nanostructures is becoming more and more important due to the requirements on magnetic, electronic and optical devices to reduce in size and dimension [1,2].

In this work we are bridging over both length and time scales by applying different suitable theoretical methods. To investigate and predict the nucleation of atomic islands on strained surfaces, a linear strain dependence of both valley and saddle site energies is implemented in the kinetic Monte Carlo (KMC) simulation model [3]. First-principle density functional theory (DFT) calculations of various material systems show that the strain dependence of both valley and saddle site energies are reasonably linear [4]. The DFT calculations indicate that the lattice sites with highest tensile strain are the most energetically favorable sites for nucleation. The periodic strain fields applied in this study are calculated based on a continuum model by Freund [5]. Periodic dislocation networks confined to the interface between the substrate and a capping layer have been reported for both metal and semiconductor structures [6,7].

In this work it is assumed that the capping layer surface is atomically flat with a periodic strain field originating from the dislocation arrangement in the interface. Experimental evidence of strain-assisted self assembly of nanopatterns has been reported for both semiconductor and metal systems [8,9]. Various aspects of strain-assisted nanopatterning of Co and Ag islands on periodically strained Pt(111) and Ag(111) surfaces, respectively, are investigated, i.e. optimal growth conditions and the effects of strain relaxation and modified step-edge barriers (i.e. Ehrlich-Schwoebel (ES) barriers [10,11]).

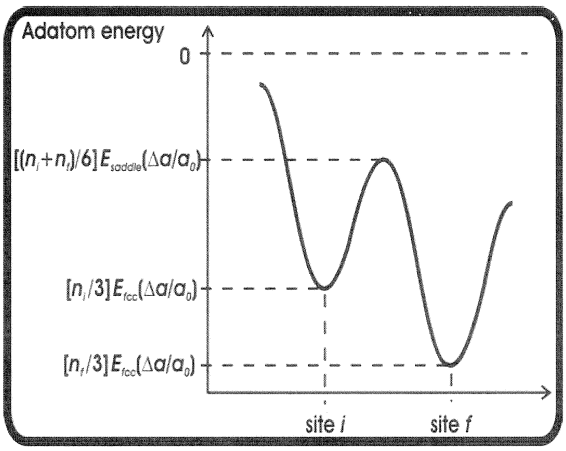

Fig. 1. Schematic potential-energy landscape showing the relationship between the energy parameters used in the kinetic Monte Carlo simulation model.

2 KINETIC MONTE CARLO SIMULATION MODEL

The kinetic Monte Carlo simulation model is a full-diffusion bond-counting model. It is a modified version of the models described in Refs. 12 an 13. In the present version of the KMC model [3], the activation energy for diffusion E depends on the lattice mismatch $\Delta a/a_0$, the initial coordination number n_i and the final coordination number n_f The following expression for E is used in the model: $E(n_i, n_f, \Delta a/a_0) = (n_i+n_f)E_{saddle}(\Delta a/a_0)/6 - n_iE_{fcc}(\Delta a/a_0)/3$, where $n_iE_{fcc}(\Delta a/a_0)/3$ is the binding energy at an fcc site and $(n_i+n_f)E_{saddle}(\Delta a/a_0)/6$ is the saddle point energy. The corresponding potential energy landscape is schematically shown in one dimension in Fig. 1. Linear energy-strain relationships are used for both fcc sites and saddle points. The hopping rate in the KMC model is

conventionally given by $\nu(n_i, n_f, \Delta a/a_0) = \nu_0 \exp(-E(n_i, n_f, \Delta a/a_0)/k_B T)$, where the attempt frequency $\nu_0 = 1\times10^{13}$ Hz, T is the substrate temperature and k_B is Boltzmann's constant. The simulations in this study are performed on surface lattices of size 512 ×256 sites if not other is stated.

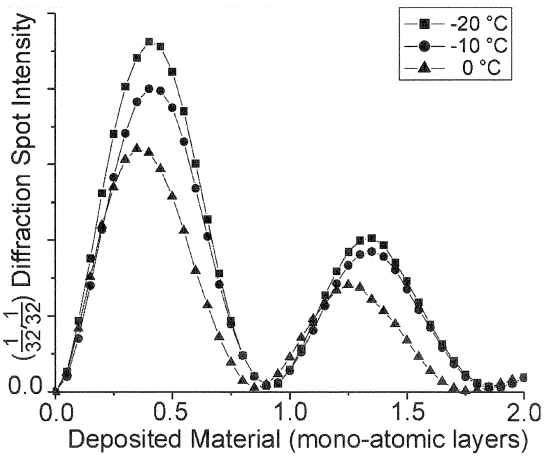

Fig. 2. The (1/32, 1/32) diffraction spot intensity vs. deposited amount of Co calculated in the out-of-phase condition between adjacent layers for the three "roughest" simulated surfaces.

3 OPTIMIZATION OF GROWTH PARAMETERS

To find the optimal conditions for nanopatterning of Co islands on periodically strained Pt(111) the Co adatom kinetics is modeled using the following DFT calculated energy-strain dependencies $E_{fcc}(\Delta a/a_0) = -4.1 - 3.8\Delta a/a_0$ [eV] and $E_{saddle}(\Delta a/a_0) = -3.8 - 2.2\Delta a/a_0$ [eV].

Three selection criteria are used to pick out the parameters giving the optimal nanopatterning. First the effective surface roughness $\langle(w - \langle w\rangle)^2\rangle$, where w is the width of the growth front, is maximized in order to obtain a pattern with multi-level high nanoislands. The purpose of the second criterion is to optimize the periodic ordering of islands. This is accomplished using kinematical diffraction calculations. The reciprocal lattice vector $\boldsymbol{K}_s$, corresponding to the strain field periodicity is used in the calculation. The maximum sensitivity to the surface morphology is obtained at the out-of-phase condition $k_z d = (2n + 1)\pi$, where d is the surface step height and n is an integer. The third criterion is to optimize the island density η_i as a function of the island diagonal length l_d for all occupied surface layers i. For a well-characterized island distribution the width of the distribution should be minimized and η_i maximized simultaneously. Applying these criteria we found the optimal nanopattern for a capping layer thickness of 9 atomic layers, T = -20 ºC and growth rate R = 0.1 ML/s. To show that T = -20 ºC gives the best nanopattern periodicity, the evolution of the most periodicity-sensitive diffraction intensity for T = -20 ºC, -10 ºC and 0 ºC (i.e. the temperatures that generated the roughest surfaces) are compared in Fig. 2. The highest intensity is obtained for T = -20 ºC; the optimal temperature for nanopatterning.

The corresponding hexagonal biaxial strain field $\varepsilon = (\varepsilon_{xx} + \varepsilon_{yy})/2$ varies between -0.9% and 2.3% with a distance of 9 nm between adjacent strain maxima, cf. Fig. 3. A representative surface image after 2 ML deposition is shown in Fig. 4(a) and the corresponding island density distribution calculated after deposition of 1 ML Co is presented in Fig. 5. The islands in layer 2 are large but have not started to coalesce yet. To act as a template for the nucleation in layer 3, a high layer 2 island density together with a large average island size and a narrow density distribution are desirable. For lower temperature the island shape becomes irregular due to low adatom diffusion and for sufficiently high temperatures the thermal energy will be so high that the strain modulation is not efficient enough to confine the adatoms to the strain maxima.

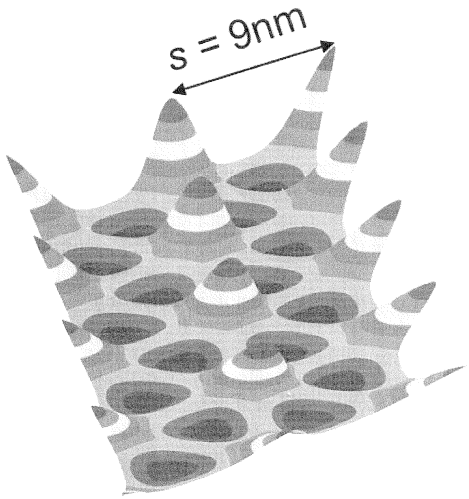

Fig. 3. The hexagonal biaxial strain field used in the Co on Pt(111) simulations. It varies between -0.9% and 2.3% with a distance of 9 nm between adjacent strain maxima.

4 STRAIN DEPENDENCE ON LAYER COVERAGE

A new parameter that we would like to call the threshold layer coverage θ_t, is introduced in order to qualitatively model the strain relaxation of partly filled layers. If a particular surface layer covers less than θ_t, the adatoms diffusing on top of that layer are not affected by any strain field. But when the coverage reaches θ_t, the adatoms diffusing on top of the layer under consideration is affected

by the strain field. Since so far in this work, only θ_t = 0 % was investigated. The evolution of the effective surface roughness for Co growth on Pt(111) with optimized growth parameters is shown in Fig. 6. The roughness degrades with increasing θ_t, however θ_t = 20 % gives almost the same roughness (and pattern quality) as θ_t = 0 % and even θ_t = 40 % yields a fairly good nanopattern. For increasing θ_t, the roughness oscillations indicate that the growth mode becomes more and more layer-by-layer.

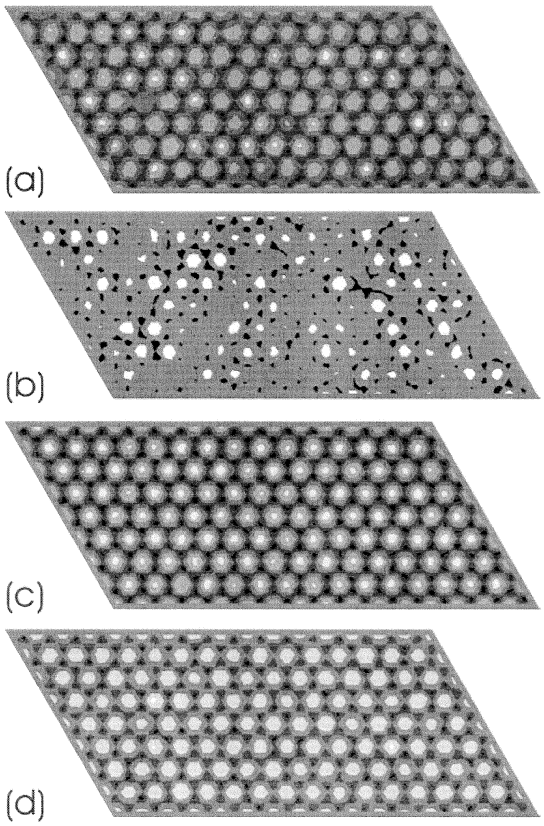

Fig. 4. Simulated surface images showing how the self assembly is influenced by ES barriers for (a) Co on Pt(111) and (c) Ag on Ag(111) compared to growth without ES barriers for (b) Co on Pt(111) and (d) Ag on Ag(111). Optimized simulation parameters are used and 2 ML is deposited in each simulation.

5 STEP-EDGE BARRIER EFFECTS

An adatom approaching a straight step edge in our KMC simulations is normally affected by an enhanced potential energy barrier due to the reduced coordination number at the step edge. The transition sites on step edges with (100) or (111) step risers are two- and one-fold coordinated, respectively. To model the effect of no ES barriers, the adatoms experience 3-fold coordination all the way to the step edge. The possibility to simulate growth with and without ES barriers allows us to qualitatively investigate the effect of surfactant mediated growth. It has been shown that surfactants can effectively reduce the ES barriers [6,14].

Representative results for the simulations of 2 ML Co grown on strained Pt(111) surfaces are shown in Fig. 4(a) for growth with ES barriers and in Fig. 4(b) for growth without ES barriers. The growth with ES barriers gives rise to a well-ordered nanopattern, however without ES barriers the growth is more layer-by-layer with only weak periodic island ordering.

To understand this mechanism better the influence of ES barriers is also simulated for growth of 2 ML Ag on periodically strained Ag(111), using R = 0.1 ML/s and T = -200 ºC, as is shown in Fig. 4(c) with ES barriers and in Fig. 4(d) without ES barriers. The energy-strain dependencies for Ag on Ag(111) are $E_{fcc}(\Delta a/a_0)$ = -2.53 – 2.8$\Delta a/a_0$ [eV] and $E_{saddle}(\Delta a/a_0)$ = -2.45 – 2.1$\Delta a/a_0$ [eV], according to Ref. 2.

The biaxial strain field ranges from -0.9 % to 2.3 % (corresponding to a 9 ML thick capping layer) for the initial Ag surface and decreases gradually for consecutive layers, e.g. the strain in the second grown layer varies between -0.8 % and 1.8 %. A comparison of the nanopatterns in Fig. 4 demonstrates that the strain modulation is more efficient for Ag on Ag(111) than for Co on Pt(111).

To compare strain-assisted growth it is possible to use the ratio, $[E_{fcc}([\Delta a/a_0]_{max}) - E_{fcc}(\Delta a/a_0 = 0)] / E_{fcc}(\Delta a/a_0 = 0)$, where $E_{fcc}(\Delta a/a_0 = 0)$ is the unstrained adatom binding energy on an unstrained fcc site and $E_{fcc}([\Delta a/a_0]_{max})$ is the corresponding binding energy on the most tensile strained fcc site. For $\Delta a/a_0$ = 2.3 %, which is the maximum lattice mismatch used for both Pt(111) and Ag(111) the ratio is

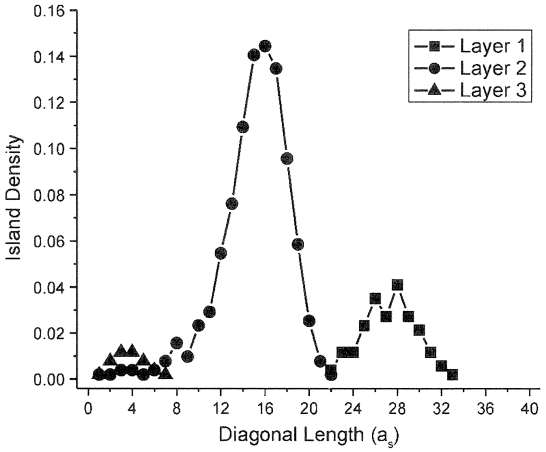

Fig. 5. Island density vs. island diagonal length after deposition of 1 ML Co, using optimized growth conditions. The corresponding simulation was performed on a lattice of size 1024×512 sites.

almost four times larger for a Ag adatom on Ag(111) than for a Co adatom on Pt(111). This results in much stronger strain influence for Ag adatoms than for Co adatoms, which is consistent with our KMC simulations.

The surface roughness evolution for 5 ML strain modulated growth of Ag on Ag(111) is shown in Fig. 7. The roughness grows monotonically for the simulations with ES barriers, but without ES barriers the roughness oscillates somewhat, indicating weak layer-by-layer growth. The roughness assuming Poisson growth, i.e. $\langle (w-\langle w \rangle)^2 \rangle = x^{1/2}$, where x is the deposited material amount in mono-atomic layers, is plotted for comparison (cf. the dotted line).

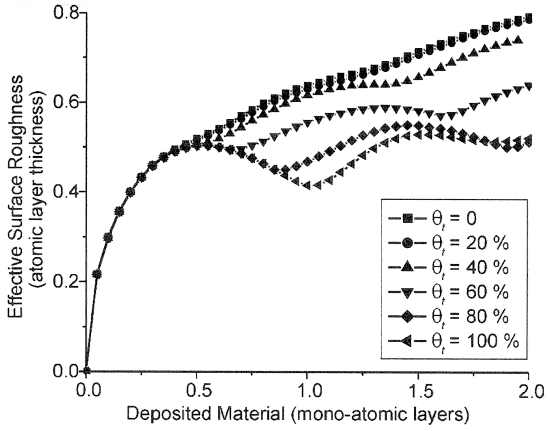

Fig. 6. The effective surface roughness vs. deposited amount of Co for various threshold layer coverage, θ_t.

6 CONCLUSIONS

Kinetic Monte Carlo simulations indicate that nucleation is favored on lattice sites with tensile strain. We predict the optimal nanopatterning condition to be very sensitive to both strain field and temperature. The strongest nanopatterning is generally achieved with significant Ehrlich-Schwoebel barriers. Our investigation shows also that the nanopatterning is just weakly strain dependent for layer coverage below ~40%. This study can be used to give guidance to optimize the experimental process.

7 ACKNOWLEDGEMENTS

We are grateful to Prof. W. Nix for valuable discussions. This work is supported by the NSF Grant EEC-0085569. The simulations were performed using the computing facilities at the Department of Physics, Karlstad University, Sweden.

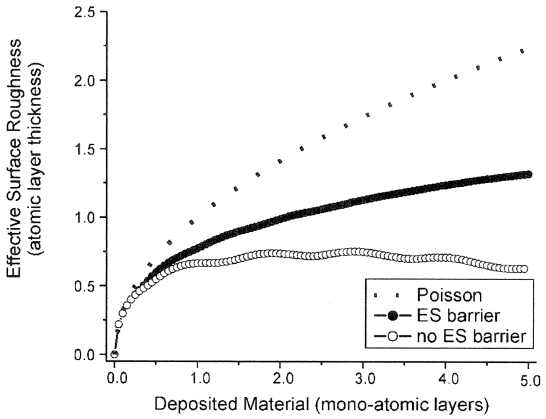

Fig. 7. Evolution of the effective surface roughness for various growth modes of Ag on Ag(111).

REFERENCES

[1] V.A. Shchukin and D. Bimberg, Rev. Mod. Phys. **71**, 1125 (1999).

[2] C. Teichert, Physics Reports **365**, 335 (2002).

[3] M. I. Larsson, B. Lee, R. F. Sabiryanov, K. Cho, W. Nix, and B. M. Clemens, in *Modeling and Numerical Simulation of Materials Behavior and Evolution*, Eds. V. Tikare, E. A. Olevsky, and A. Zavaliangos, (Mater. Res. Soc., Pittsburgh, 2002) Vol. **731**, 269.

[4] C. Ratsch, A. P. Seitsonen and M. Scheffler, Phys. Rev. B **55**, 6750 (1997).

[5] L. B. Freund, Adv. in Appl. Mechanics **30**, 1 (1994).

[6] H. Brune, Surf. Sci. Rep. **31**, 121 (1998).

[7] M. Horn von Hoegen, Z. Kristallogr. **214**, 1 (1999).

[8] B. Voigtländer and Theuerkauf, Surf. Sci. **461**, L575 (2000).

[9] K. Bromann, M. Giovannini, H. Brune, and K. Kern, Eur. Phys. J. D **9**, 25 (1999).

[10] G. Ehrlich and F. G. Hudda, J. Chem. Phys. **44**, 1039 (1966).

[11] R. L. Schwoebel and E. J. Shipsey, J. Appl. Phys. **37**, 3682 (1966).

[12] M. I. Larsson, Phys. Rev. B **64**, 115428 (2001).

[13] M. I. Larsson, Phys. Rev. B **56**, 15175 (1997).

[14] H. A. van der Vegt, H. M. van Pinxteren, M. Lohmeier, E. Vlieg, and J. M. C. Thornton, Phys. Rev. Lett. **68**, 3335 (1992).